

Elastic Scattering Reaction of ${}^4\text{He}+{}^{10}\text{B}$ on Partial Wave Scattering Matrix, Differential Cross-Section and Reaction Cross-Section at Laboratory Energies of 5-15 Mev: An Optical Model Analysis.

Arusei Geoffrey Kipkorir^{1*}, Yegon Geoffrey Kipkoech¹, Samwel K.Rotich¹, [Ronoh K.Nixon² R.K.Koech³ and D.K Choge³

1. Department of Physics, Moi University, P.O Box 3900, Eldoret (Kenya)
E-mail: aruseig@yahoo.com, yegonkipgeff@gmail.com, samkrotich@yahoo.com.
2. Department of Mathematics and Computer Science, Moi University, P.O Box 3900, Eldoret (Kenya)
E-mail: nronoh@hotmail.com
3. Department of Physics, University of Eldoret, P.O Box 1125, Eldoret (Kenya)
E-mail: rkkoech09@gmail.com, cdismas2004@yahoo.com.

Abstract

The nuclear optical model has been used in the analysis of elastic scattering for the reaction ${}^4\text{He}+{}^{10}\text{B}$. This model has six optical parameters; the depth, Coulomb radius and the diffuseness on both the real part and imaginary part potentials. Out of the six, five parameters were chosen and for this case diffuseness parameter on the imaginary part was kept constant. The five parameters were used to calculate the partial wave S-matrix, the differential cross section and the reaction cross section as a ratio to Rutherford cross section. The partial wave scattering data was obtained basing on the quantum mechanical optical code for all the stated Laboratory energies. The angular distribution for the reaction ${}^4\text{He}+{}^{10}\text{B}$ for both reaction cross section to the Rutherford cross-section and differential cross section ranging from centre of mass angles (θ_{cm}) of $0^\circ - 180^\circ$ were also obtained for all the energies, ($E_{Lab} = 5, 7, 12$ and 15 MeV) and whose data and graphs are presented.

Key words: Differential cross-section, Reaction cross-section and Partial scattering matrix.

1. Introduction

Nuclear reactions and nuclear scattering are often used to measure the properties of nuclei, both in industry and academia for example; Reactions that exchange nucleons can be used to measure the binding energies of excitation, quantum numbers of energy levels, and transition rates between levels. A particle accelerator, which produces a beam of high-energy charged particles, creates these reactions when they strike a target nucleus. Nuclear reactions can also be produced in nature by high-energy particles from cosmic rays, for instance in the upper atmosphere or in space [1].

In order for a nuclear reaction to occur, the nucleons in the incident particle, or projectile, must interact with the nucleons of the target. This energy should be high enough to overcome nuclear potential barrier. Early experiments by Rutherford [2] used low-energy alpha particles from naturally radioactive materials like Americium-241 to bounce off target atoms and thus enabled the measurement of the size of the target nuclei. When a collision occurs between the incident particle and a target nucleus, either the beam of particles scatter elastically leaving the target nucleus in its ground state or the target nucleus is internally excited and subsequently decays by emitting radiation or nucleons.

A specific reaction is studied by measuring the angles and kinetic energies of the reaction products for example the kinematics variables [3]. The most important quantity of interest for a specific set of kinematics variable is the reaction cross section (σ) which is a measure of the probability for a particular reaction to occur.

2. Theory

A nuclear reaction is initiated by bombarding target nuclei with a beam of nucleons or nuclei. In the early days, it was common to use a beam of α -particles from radioactive decay but nowadays the beam of particles comes from some sort of particle accelerator as shown in the figure below.

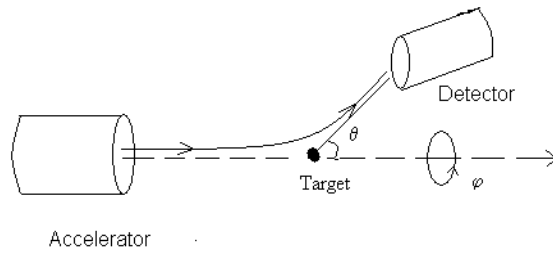


Fig 2.1 Accelerator

Where θ is the scattering angle and φ is the coherent scattering cross section.

A general nuclear reaction equation (2.1) is written as



or simply $A(a,b)B$, where a is the bombarding particle (projectile) and A the target nucleus, B the residual nucleus and b , is the outgoing particle or the nucleus which is detected.

Reactions of the type given by equation (2.1) are governed by the usual conservation laws of energy, linear momentum and angular momentum. In addition, charge and the total number of nucleons will also be conserved whenever a nuclear reaction takes place.

There is always a difference in mass between initial and final states given by the expression

$$Q = [(M_A + M_a) - (M_B + M_b)]c^2, \quad 2.2$$

where Q is the heat generated, M_A is the mass of the target nucleus, M_a is the mass of the bombarding particle, M_B is the mass of the residual nucleus, M_b is the mass of an outgoing particle while c is the speed of light.

An alternative definition of Q can be obtained by using the conservation of energy during the reaction process. Thus, if the kinetic energies in the laboratory system of the different particles and nuclei taking part in the reaction are denoted by T_i (for target nucleus A , being at rest, $T_A = 0$), then conservation of energy requires that,

$$M_A c^2 + M_a c^2 + T_a = M_B c^2 + T_B + M_b c^2 + T_b, \quad 2.3$$

where M are masses of particles A, a, B and b , and T are the kinetic energies of particles a, B and b , respectively. On combining equations (3.2) and (3.3) gives

$$Q = T_B + T_b - T_a. \quad 2.4$$

Q values can be positive implying exothermic reactions or negative for endothermic reactions and will be zero in the case of an elastic scattering process of the type



If Q is negative, energy conservation requires that kinetic energy must be brought in by the bombarding particle if the reaction is to take place. In the laboratory system, this energy must be larger than the $|Q|$ values because conservation of momentum does not allow the residual nucleus and the outgoing particle to be at rest in the laboratory frame of reference.

Denoting the speed of particles a and A in this system as V_a and V_A , respectively, then the conservation of linear momentum becomes

$$M_a V_a + M_A V_A = 0 \text{ giving } V_A = -\frac{M_a V_a}{M_A}. \quad 2.6$$

In the centre of mass system, the total kinetic energy with reference to equation (2.6) becomes

$$\begin{aligned} T &= \frac{1}{2} M_a V_a^2 + \frac{1}{2} \frac{M_a^2}{M_A} V_a^2 \\ &= \frac{1}{2} M_a V_a^2 \left[1 + \frac{M_a}{M_A} \right]. \end{aligned} \quad 2.7$$

In the laboratory system when the target nucleus is at rest, the total kinetic energy is given by

$$T' = \frac{1}{2} M_a V_a'^2, \quad 2.8$$

where V_a' is the speed of particle a in this system. But V_a' is the relative velocity of particle a and A given as

$$V_a' = V_a - V_A. \quad 2.9$$

Substituting this expression for V_a' in equation (2.8) and using equation (2.6) then gives

$$T' = \frac{1}{2} M_a V_a^2 \left(1 + \frac{M_a}{M_A} \right)^2. \quad 2.10$$

On comparing equations (2.7) and (2.10) we finally obtain

$$T' = T \left(1 + \frac{M_a}{M_A} \right). \quad 2.11$$

The condition for an endothermic reaction to proceed requires that $T \geq |Q|$ or using equation (2.10) becomes

$$T' \geq |Q| \left(1 + \frac{M_a}{M_A} \right). \quad 2.12$$

2.1.0 Reference frames and transformational laws

The cross sections of nuclear reactions are always measured in the laboratory coordinate system where the target is at rest. But it is more fundamental and more convenient to analyze them relative to the centre of mass of the projectile and the target namely in the centre of mass system. The transformation equations are obtained from the laws of conservation of energy and momentum in the non-relativistic case.

The two fundamental quantities that result from the transformation are the reduced mass ξ and the energy E_{cm} in the centre of mass frame. In terms of the projectile and the target masses, M_P and M_T and the projectile energy in the lab frame, E_{Lab} , these quantities are given by:

$$\xi = \frac{M_P M_T}{M_P + M_T}. \quad 2.13$$

$$\text{and } E_{cm} = \frac{M_T}{M_P + M_T} E_{Lab}. \quad 2.14$$

The relative velocity in the centre of mass frame is the same as that in the laboratory frame of reference.

2.2 Optical model potential

Most of the data for elastic particle scattering have been analyzed in terms of the optical model in which the projectile-target nucleus interaction is represented by a complex potential. To describe a nuclear reaction between two nuclei A_1 and A_2 , the Schrödinger equation has to be written for each nucleon of the system. Each nucleon is in a potential well created by the other $(A_1 + A_2 - 1)$ nucleons. In the frame of the optical model [4], all the interactions between the nucleons of the projectile and the nucleons of target are replaced by an average and central interaction $V(r)$ between the projectile and the target in their ground states. The equation to be solved becomes:

$$H\psi = \left(-\frac{\hbar^2}{2\xi} \nabla^2 + V(r) \right) \psi = E\psi. \quad 2.15$$

With $\xi = \frac{A_1 A_2}{A_1 + A_2}$ being the reduced mass of the system, A 's are the atomic masses and r the distance

between the two nuclei mass center. The optical model used to describe the interaction between two nuclei is inspired by the optical phenomenon which can be characterized by a complex index corresponding to the diffraction phenomenon and the imaginary part to the refraction of the incident wave. The averaged nuclear potential $V(r)$ can then be written as: $V(r) = U(r) + iW(r)$, 2.16

where $U(r)$ is the real part of the potential and represents the elastic scattering that is a reflection of the incident wave. The imaginary part $W(r)$ is introduced to take into account the other reactions which can occur, that is, there is an absorption of the incident wave before it is re-emitted. $W(r)$ simulates the loss of flux due to inelastic collisions.

3. METHODOLOGY

This work involved the study of the ${}^4\text{He}+{}^{10}\text{B}$ nuclear reaction using the optical model [5,6]. All calculations were carried out using Java applet program executed through an applet viewer or a java capable browser such as Microsoft internet explorer [7].

The experimental results were in-built while the theoretical results were obtained by varying the optical model parameters such as the depth of real part potential U_0 , depth of imaginary part potential W_0 , radius of nucleus i.e, r_0 (real) and r_i (imaginary) as well as the diffuseness parameters a for both real and imaginary parts for energies varying from 5-15 MeV. In each case five parameters were chosen at once out of six, three on the real part and three on the imaginary part. The data obtained were analyzed and graphs plotted using the origin software [8].

4. RESULTS AND DISCUSSIONS

This chapter presents the results obtained in this study whereby the trends are discussed, as well as observations and accounts of specific phenomena being presented.

Figure 4.1 shows a plot of the partial wave scattering matrix with the orbital angular momentum L .

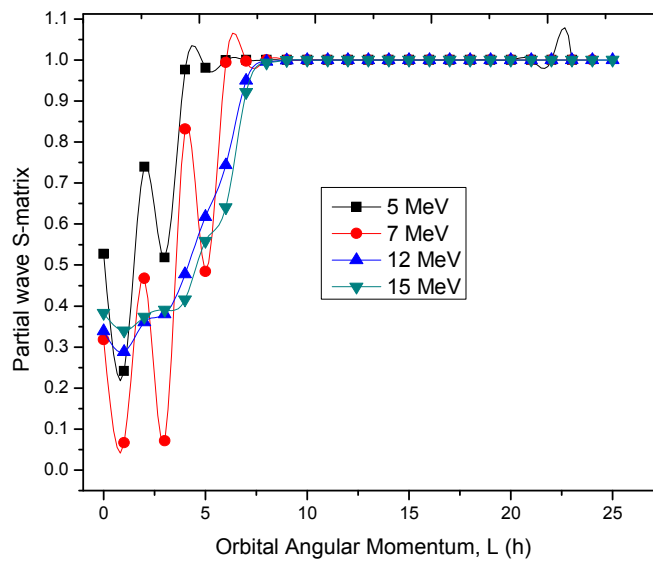


Figure 4.1: Partial wave S-matrix variation with the orbital angular momentum L for the reaction ${}^4\text{He}+{}^{10}\text{B}$ at $E_{Lab} = 5, 7, 12$ and 15 MeV.

Figure 4.1 show that the values of $|S_L|$ are approximately 0.527, 0.318, 0.339, 0.383 at $L = 0$ for incident energies $E_{Lab} = 5, 7, 12$ and 15 MeV, respectively. It is further observed that initially the values of $|S_L|$ fluctuates significantly for values of L upto approximately 6.0 and below, and then increases rapidly as the L values becomes larger, finally reaching a value of 1. This value is however attained much faster for low energies when compared to the higher ones. $|S_L|$ at $L = 0$ is interpreted as complete absorption and $|S_L|=1$ as complete reflection, where $|S_L|$ is the modulus of the scattering matrix element referred to as the reflection coefficient. The fluctuation of the partial wave S-matrix noted at a value of $L \cong 22.5$ is considered to be an anomaly since the maximum value of $|S_L|=1$ which is complete reflection. It is important to note that

$|S_L| \neq 0$ but only approaches zero, meaning that there is no complete absorption.

Figure 4.2: Shows the variation of the differential cross section $\left(\frac{d\sigma}{d\Omega}\right)$ plotted with centre of mass angles (θ_{cm}) for the reaction ${}^4\text{He}+{}^{10}\text{B}$ at $E_{Lab} = 12\text{ MeV}$.

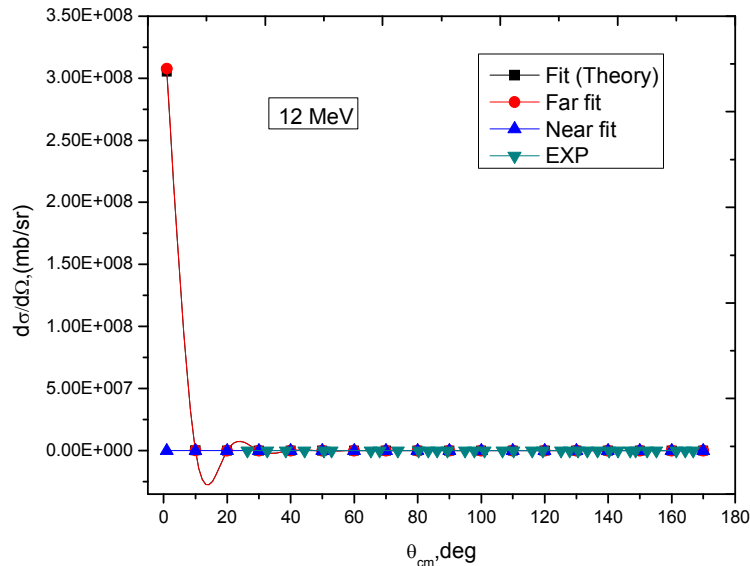


Figure 4.2: Differential cross section $\left(\frac{d\sigma}{d\Omega}\right)$ for the reaction ${}^4\text{He}+{}^{10}\text{B}$ at $E_{Lab} = 12\text{ MeV}$.

In this case, the highest point appears at 0.022° and the minimum at a centre of mass angle of 14.123° (all these values were obtained from the graph using data reader in the Origin computer program). In this graph, no good agreement is established for small angles between theory and experimental values, but there is good correlation between experimental and theory for angles greater than 30° . This is attributed to the response of the strong Coulomb force.

Fig 4.3 Shows the variation of the differential cross-sections $\left(\frac{d\sigma}{d\Omega}\right)$ with the centre of mass angles (θ_{cm})

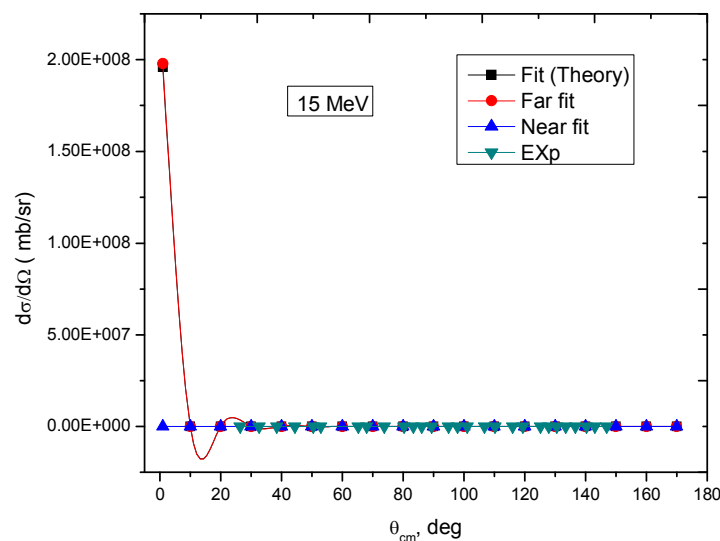


Figure 4.3:-Differential cross section $\left(\frac{d\sigma}{d\Omega}\right)$ for the reaction ${}^4\text{He}+{}^{10}\text{B}$ at $E_{Lab} = 15\text{ MeV}$.

The general trend in Figure 5.6 is similar to that observed for lower energies i.e 5, 7 and 12 MeV. At this relatively high energy, the highest value of $\frac{d\sigma}{d\Omega}$ occurs at 0.022° while the minimum is found at 13.518° .

In summary the plots of the differential cross section with angular distribution at all these energies considered in this study show the same trend for both theoretical and experimental results while those of the far fit and the theory (fit) graphs re-trace the same path. From the graphs, it is established that the differential cross section is high at lower scattering angles and smaller for larger ones. Just like in the previous cases, this is attributed to the existence of a greater repulsive force as the incident particle approaches the target nuclei due to the existence of the Coulomb force associated with the charge. In this case, the trajectories that are deflected back belong to the near side. This again is associated with the small impact parameter and strong repulsive force from the nucleus whereas those scattered to the opposite side of the target are the far-side ones and these are due to large impact parameter and small repulsive force. The graphs of the differential cross section are found to decrease exponentially with increase in the scattering angle but it is also seen that at scattering angles close to zero, the magnitude of the differential cross section decreases with increase in the laboratory energies 5 MeV, 7 MeV, 12 MeV and 15 MeV in that order.

Fig 4.4 shows a plot of the reaction cross-section $\left(\frac{\sigma}{\sigma_R}\right)$ with the centre of mass angles (θ_{cm})

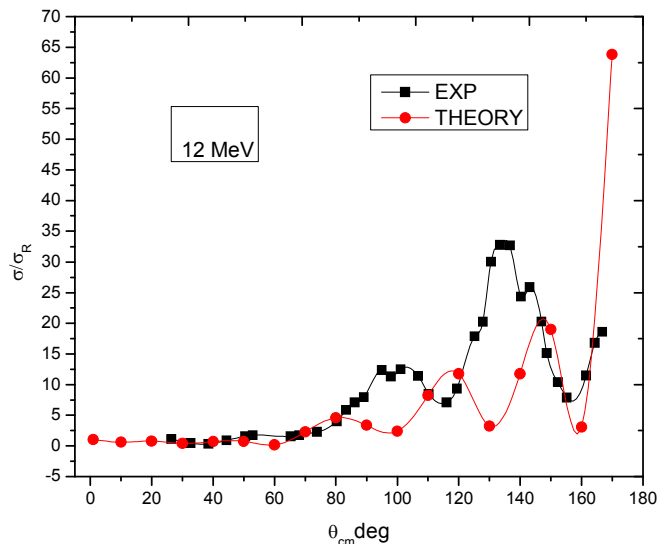


Figure 4.4: Calculated angular distribution (circled symbols) of elastic scattering ${}^4\text{He}+{}^{10}\text{B}$ at $E_{Lab} = 12$ MeV.

For this graph (Figure 4.4) the minima for theory occur at centre of mass angles θ_{cm} of 97.197° , 129.747° and 158.445° while the maxima occurs at 79.751° , 119.098° and 147.797° . The red curve (circled symbols) shows the theoretical results of the optical model represented by the word THEORY while the experimental results are represented by the black curve (square symbols) denoted as EXP. There appears to be a shift in the extrema. It is clear from the plot that theory does not quite follow experimental results for all scattering angles especially those between 90° and 150° , whereas there is similarity at smaller angles below 90° . As noted before, a maximum or minimum point in the ratio of the reaction cross-section σ/σ_R occurs when σ is large and minimum for small values of σ , assuming that the Rutherford cross-section σ_R is fixed.

Fig 4.5 shows the variation of the reaction cross-section $\left(\frac{\sigma}{\sigma_R}\right)$ with the centre of mass angles (θ_{cm}) for 15 MeV.

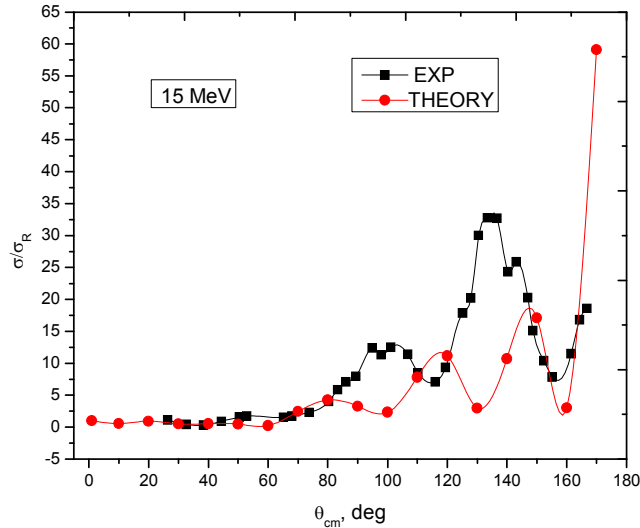


Figure 4.5: Calculated angular distribution (circled symbols) and experimental values (squared symbols) of elastic scattering ${}^4\text{He}+{}^{10}\text{B}$ at $E_{Lab} = 15$ MeV.

Figure 4.5 shows a graph of the reaction cross-section expressed as a ratio to Rutherford reaction cross-section against the centre of mass angles. In this high energy range, the minima of the theory occurs at the angles of 99.085° , 129.747° and 158.445° , while the maxima occurs at 79.751° , 117.814° and 147.192° . Incidentally the values for maxima and minima for this energy range occurs at almost the same centre of mass angles as for the 12 MeV energy range. The highest value of $\frac{\sigma}{\sigma_R}$ is found at

169.698° . The red colour in the curve shows the theoretical results (circled symbols) while the black curve shows the experimental results (square symbols) of the optical model.

Like in previous cases, this plot shows that theory does not quite follow experimental results between the scattering angles of 90° and 140° , whereas the trend is followed for angles falling outside of this range.

Overall an oscillatory trend is observed in the plot of $\frac{\sigma}{\sigma_R}$ versus θ_{cm} for energies considered in this study. It

observed that at lower centre of mass angles, the reaction cross sections are small and have similar trend for all the energies unlike at large angles whose reaction cross section is large and oscillates highly with increase in the energies. Nonetheless, the trend is still followed between the energies 7, 12 and 15 MeV. This behaviour is due to the fact that at small angles, the impact parameter is high and the Coulomb force is small while for large angles the Coulomb force is stronger at small impact parameters. This applies for small centre of mass angles between $1^\circ - 60^\circ$ and large ones between $60^\circ - 170^\circ$.

5. Conclusions

The nuclear reaction ${}^4\text{He}+{}^{10}\text{B}$ has been analyzed through elastic scattering at laboratory energies E_{Lab} of 5, 7, 12 and 15 MeV using the optical model with the aim of obtaining useful nuclear reaction data relevant to the nuclear industry. The basic features of colliding nuclei including the impact parameter, scattering angle and reaction cross sections have been obtained. Optical model parameters like the depth of real part potential U_0 , depth of the imaginary part potential W_0 , nuclear radius r_0 (real) and r_i (imaginary) as well as the diffuseness a for both real and imaginary parts for different laboratory energies for the system ${}^4\text{He}+{}^{10}\text{B}$ nuclear reaction have been extracted. The optical model interaction potential, nuclear elastic scattering angular and energy

distribution, and the observable quantities such as differential cross section, partial wave scattering matrix and the reaction cross section as a ratio to the Rutherford cross-section were also extracted. A plot of the optical model interaction potential shows a deep real (reflective) part U (MeV) and weakly absorptive imaginary part W MeV while for partial wave S-matrix, it fluctuates at lower values of orbital angular momenta L and increases rapidly at larger values of L until it attains maximum at the point where $|S_L| = 1$ which is interpreted to have a complete reflection. The theoretical results of the angular distribution of elastic scattering at different laboratory energies have yielded a good agreement with the corresponding experimental data in the reaction cross-section, although some minor disagreements with the differential cross section at lower centre of mass angles are noted.

References

- [1] Matis H. and Berkeley, "A Guide to the Nuclear Science Wall Chart," Contemporary Physics Education Project, California, USA (2003).
- [2] Asimov I. and Bach, D. F, "Atom-Journey across the Sub Atomic Cosmos, Penguin USA, (1992).
- [3] Lilley J. S. "Nuclear Physics," University of Manchester England (2008).
- [4] Hodgson P. E., "The Optical Model of Elastic Scattering," Oxford University Press, London, UK (1963).
- [5] Hodgson P. E., "Nuclear Reactions and Nuclear Structure," Clarendon Press UK (1971).
- [6] Satchler G. R., "Direct Nuclear Reactions," Oxford University Press, New York, USA (1983).
- [7] Broglia R. A And Winther A., "Heavy Ion Reactions; Elastic and Inelastic Reactions," Benjamin, Reading (1981).
- [8] Ian. J "Nuclear reactions for astrophysics, principles, calculation and application of low-energy reaction," michigan state University 2009

This academic article was published by The International Institute for Science, Technology and Education (IISTE). The IISTE is a pioneer in the Open Access Publishing service based in the U.S. and Europe. The aim of the institute is Accelerating Global Knowledge Sharing.

More information about the publisher can be found in the IISTE's homepage:

<http://www.iiste.org>

CALL FOR JOURNAL PAPERS

The IISTE is currently hosting more than 30 peer-reviewed academic journals and collaborating with academic institutions around the world. There's no deadline for submission. **Prospective authors of IISTE journals can find the submission instruction on the following page:** <http://www.iiste.org/journals/> The IISTE editorial team promises to review and publish all the qualified submissions in a **fast** manner. All the journals articles are available online to the readers all over the world without financial, legal, or technical barriers other than those inseparable from gaining access to the internet itself. Printed version of the journals is also available upon request of readers and authors.

MORE RESOURCES

Book publication information: <http://www.iiste.org/book/>

Recent conferences: <http://www.iiste.org/conference/>

IISTE Knowledge Sharing Partners

EBSCO, Index Copernicus, Ulrich's Periodicals Directory, JournalTOCS, PKP Open Archives Harvester, Bielefeld Academic Search Engine, Elektronische Zeitschriftenbibliothek EZB, Open J-Gate, OCLC WorldCat, Universe Digital Library, NewJour, Google Scholar

